

THIS REPORT HAS BEEN DELIMITED
AND CLEARED FOR PUBLIC RELEASE
UNDER DOD DIRECTIVE 5200.20 AND
NO RESTRICTIONS ARE IMPOSED UPON
ITS USE AND DISCLOSURE,

DISTRIBUTION STATEMENT A

APPROVED FOR PUBLIC RELEASE;
DISTRIBUTION UNLIMITED.

AD919346

Report USAAMRDL-TR-74-13



EVALUATION OF FUEL FOG INERTING CONCEPTS

**Russell Laustsen, Robert Bristow
The Boeing Company
Seattle, Washington 98100**

April 1974

Final Report

**DDC-RPAPLWD
JUN 3 1974
C**

Distribution limited to U. S. Government agencies only; test and evaluation; April 1974. Other requests for this document must be referred to the Eustis Directorate, U. S. Army Air Mobility Research and Development Laboratory, Fort Eustis, Virginia 23604.

Prepared for

**EUSTIS DIRECTORATE
U. S. ARMY AIR MOBILITY RESEARCH AND DEVELOPMENT LABORATORY
Fort Eustis, Va. 23604**

EUSTIS DIRECTORATE POSITION STATEMENT

A test program was conducted in which a very simple fog system was completely effective in preventing ullage ignition by electric match. However, other ignition sources were not tested. Subsequent to this contractual effort, the system was evaluated and found to be ineffective in both Government-conducted caliber .30 M1 incendiary tests and contractor-conducted incendiary gunfire simulator tests. Therefore, in spite of the success of the system against an electric match ignitor, the value of the condensate-formed fuel fog concept has not been firmly established. Results of the gunfire tests will be given in a subsequent report.

This report has been reviewed by this Directorate and is considered to be technically sound.

The technical monitor for this contract was Mr. Charles M. Pedriani of the Military Operations Technology Division.

DISCLAIMERS

The findings in this report are not to be construed as an official Department of the Army position unless so designated by other authorized documents.

When Government drawings, specifications, or other data are used for any purpose other than in connection with a definitely related Government procurement operation, the United States Government thereby incurs no responsibility nor any obligation whatsoever; and the fact that the Government may have formulated, furnished, or in any way supplied the said drawings, specifications, or other data is not to be regarded by implication or otherwise as in any manner licensing the holder or any other person or corporation, or conveying any rights or permission, to manufacture, use, or sell any patented invention that may in any way be related thereto.

Trade names cited in this report do not constitute an official endorsement or approval of the use of such commercial hardware or software.

DISPOSITION INSTRUCTIONS

Destroy this report when no longer needed. Do not return it to the originator.

Unclassified

SECURITY CLASSIFICATION OF THIS PAGE (When Data Entered)

DD FORM 1 JAN 73 1473 EDITION OF 1 NOV 65 IS OBSOLETE

Unclassified

SECURITY CLASSIFICATION OF THIS PAGE (When Data Entered)

Unclassified

SECURITY CLASSIFICATION OF THIS PAGE(When Data Entered)

20. Continued

provided inerting over the complete range of ullage-space temperatures tested (+60°F to -55°F). Further findings for the 6-cubic-foot ullage space (over liquid JP-4 fuel) were that 1.0-gph nozzles were sufficient but 0.4-gph nozzles were not, neither single hot nor single cold nozzles were sufficient, and inerting would not occur for all ullage conditions except when both hot and cold nozzles were used. It was found that the hot and cold spray temperature differentials could each be at least as low as 5°F.

In addition, a fuel fogging preliminary design for the AH-1G Cobra helicopter is included.

Unclassified

SECURITY CLASSIFICATION OF THIS PAGE(When Data Entered)

TABLE OF CONTENTS

	<u>Page</u>
LIST OF ILLUSTRATIONS	iv
INTRODUCTION	1
DISCUSSION.	2
Theory of Condensation-Formed Fuel Fog.	2
Flammability	2
Vapor Pressure of Mist Droplets	3
Fuel Mist Droplet Size Requirements	6
Formation of Fog Particles - Embryos.	6
Mechanism of Embryo Formation	10
Fuel Fog Testing.	12
Test Arrangement.	12
Test Results.	19
Design Application.	24
CONCLUSIONS	30
RECOMMENDATIONS	31
LITERATURE CITED.	32
APPENDIXES.	33
I. Test Data	33
II. Thermodynamic Treatment of Condensation- Formed Embryos.	36

LIST OF ILLUSTRATIONS

<u>Figure</u>	<u>Page</u>
1 Absolute Limits of Flammability for Aviation Gasoline Grade 100/130 Vapor-Air Mixtures at $78^{\circ} +1^{\circ}\text{F}$	4
2 Saturated Limits of Flammability of Aviation Gasoline Grade 100/130 Vapor-Air Mixtures.	4
3 Calculation of Vapor From Fuel Mist Droplets	7
4 Calculation of Shift in Upper Flammability Limit Which Is Theoretically Possible as a Function of Mist Droplet Diameter	8
5 Size of Things	9
6 Test Arrangement - Air Brush Nozzles	13
7 Test Arrangement - Oil Burner Nozzles.	14
8 Electric Match	16
9 Test Arrangement Schematic	17
10 Test Arrangement	18
11 Single-Nozzle Test Results	20
12 0.4, 0.4 Nozzle Test Data	21
13 0.4, 1.0 Nozzle Test Results	22
14 1.0, 1.0 Nozzle Test Results	23
15 AH-1G Fuel System Schematic	25
16 Fuel Fogger Preliminary Design	27
17 AH-1G Cobra Fuel Fogger Installation	29
18 Comparison of Evaporation Potential for Two Different Embryo Diameters	42

INTRODUCTION

Aircraft fuel tank ullage spaces represent one of the major areas vulnerable to small-arms and antiaircraft fire. This vulnerability arises because, when the fuel vapors are in the flammable region, sufficient pressure can be generated by the burning vapor to rupture the fuel cell. Many attempts have been made to make the ullage space inert. These have included reticulated foam, nitrogen inerting, catalytic burners, engine exhaust gases, and various active vapor explosion suppression schemes. All of these techniques have suffered from problems such as a weight, cost, volume, reliability, etc. For this reason, the search for a satisfactory means of vapor space inerting technique continues.

A scheme for inerting vapor spaces not mentioned above involves using condensation-formed fuel fog to drive the fuel/air ratio into the overrich region. Past efforts to make this technique work have met with failure. However, a breakthrough in the development of a theory to describe how fuel fog inerting works has led to a new approach. This report presents the theory of condensation-formed fuel fog and describes the results of a series of tests designed to demonstrate the feasibility of using fuel fog for inerting fuel tanks.

DISCUSSION

Three aspects of fuel fogging were studied during this program: theory, test and application. Each of these areas is discussed in the following paragraphs. In addition, a thermo-dynamic treatment of condensation-formed embryos is included in Appendix II.

THEORY OF CONDENSATION-FORMED FUEL FOG

Following is a discussion of the theory upon which the test program was based. The discussion starts with a section on fuel vapor flammability. It is shown that flammability depends on vapor pressure and that vapor pressure in the region around fuel droplets depends on droplet size. It is then shown that only very small droplets (droplet embryos) can significantly change the vapor pressure. Finally, the mechanism of embryo formation is discussed.

Flammability

Vulnerability of the ullage space in an aircraft fuel tank relates directly to the flammability of the vapor present at the time of introduction of an ignition source. Flammability relates to the process of fuel combustion which requires that fuel must be vaporized and then mixed with oxygen followed by reaction which is activated by an ignition source. Whether or not the reaction will propagate depends on whether the vapor composition at the time and place of ignition is within the flammability limits.

The vapor composition can be altered from that which is considered to be normal. This may occur when fuel mist exists in the vapor space. Under certain conditions of temperature difference, very small molecular clusters called embryos are generated. Because of the large surface-to-volume ratio of the embryos, surface tension effects cause an increase in bulk vapor pressure. Thus the vapor composition becomes richer in fuel vapor.

The fundamental basis to which all of the information gained from this study can be related is the combustion process itself. For combustion to occur, a fuel must first be vaporized. The vapor formed must then migrate to a zone where it can mix with an oxidant to form a flammable mixture, and subsequently react if ignited.

Flammability limits which are expressed as a fuel vapor concentration in air are related to this concept. These limits are called absolute limits. An example is shown in Figure 1.

Usually flammability limits are expressed in terms of temperature, and this leads to some confusion. An example is shown in Figure 2 on the same fuel used for Figure 1.

The temperature values in Figure 2 correspond to fuel concentration values in an environment which includes only air, fuel vapor, and liquid fuel. In an environment which includes mist droplets which cause an increase in vapor pressure with no increase in temperature, the "temperature flammability" limits do not apply.

However, in terms of fuel vapor concentration, the absolute flammability limit relationships still apply to the conditions existing at the time and place where ignition and combustion occur.

At this point it should be clear that flammability of the vapor space being considered depends on the fuel vapor concentration which is a function of vapor pressure only. Thus the effectiveness of the condensation-formed fuel fog concept is related to the fact that the normal vapor pressure is changed by conditions existing within the fog.

Vapor Pressure of Mist Droplets

The following is taken from Reference 3. A more rigorous derivation of the final equation in this section is presented in Appendix II.

The vapor pressure of a liquid is greater when it is in the form of small droplets than when it has a plane surface. This was first deduced by Lord Kelvin.

If a liquid distills from a plane surface to a droplet, the droplet must increase in size and also in surface area. This requires expenditure of work against the surface tension.

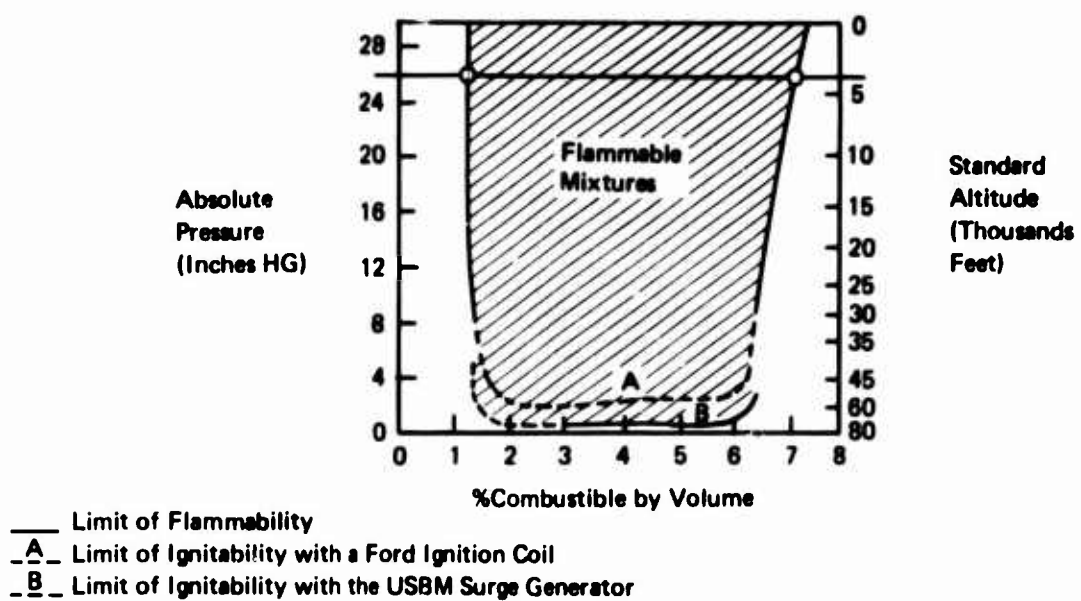


Figure 1. Absolute Limits of Flammability for Aviation Gasoline Grade 100/130 Vapor-Air Mixtures at $78^{\circ} \pm 1^{\circ}\text{F}$.

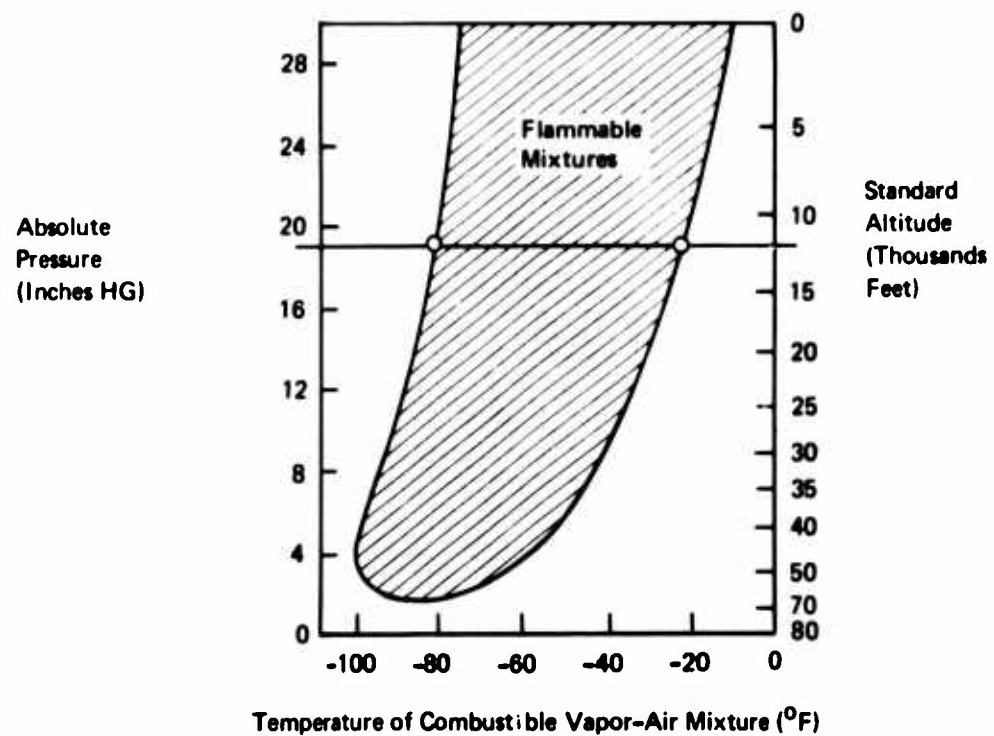
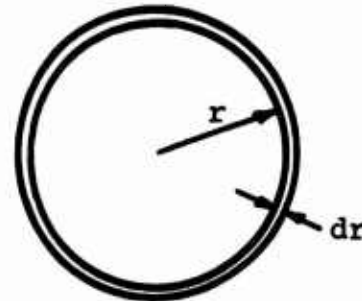


Figure 2. Saturated Limits of Flammability of Aviation Gasoline Grade 100/130 Vapor-Air Mixtures.

Consider a spherical droplet whose radius grows from r to $r+dr$.



The increase in surface area is from $4\pi r^2$ to $4\pi (r + dr)^2$, which is $4\pi (r^2 + 2rdr) - 4\pi r^2$ or $8\pi r dr$. Thus the corresponding increase in surface free energy is $8\pi r \gamma dr$ where γ is the surface tension.

If dn moles of liquid were distilled from the plane surface whose vapor pressure is P_0 to the droplet whose vapor pressure is P , the free-energy change would be given by the equation

$$F_2 - F_1 = \Delta F = RT \ln \frac{P_2}{P_1} = dn RT \ln \frac{P}{P_0}$$

Equating the free energy changes, we have

$$dn RT \ln \frac{P}{P_0} = 8\pi r \gamma dr$$

but $dn = 4\pi r^2 dr \frac{\rho}{M}$

where ρ = density

M = molecular weight.

Therefore,

$$4\pi r^2 dr \frac{\rho}{M} RT \ln \frac{P}{P_0} = 8\pi r \gamma dr$$

or $\ln \frac{P}{P_0} = \frac{2 M \gamma}{RT \rho r}$

where $R = 8.3144 \times 10^7$ ergs/deg mole

$T = ^\circ K$

$r = cm$

$\rho = grams/cm^3$

$\gamma = dynes/cm$

Fuel Mist Droplet Size Requirements

At this point, concern must be shown for the actual droplet size which must exist to cause an appreciable increase in vapor pressure according to the above equation. To show this, a calculation has been made for JP-4. The results are shown in Figure 3. Figure 4 shows the theoretical relationship of droplet size and the extent to which the upper flammability limit can be decreased for JP-4 and JP-5. Figure 5 shows a comparison of the fuel mist area of interest, 10^{-2} to 10^{-3} microns, with other objects (Reference 2).

Formation of Fog Particles - Embryos

Mist droplets can be formed in two ways: they can grow from vapor molecules by condensation, or they can be formed in special ways from bulk fluid.

Particles formed by condensation may be as much as 1000 times smaller than those formed mechanically. Since an extremely small droplet size (see Figure 4) is required to appreciably affect flammability limits, condensation droplets are of utmost importance.

In fact, condensation is the only means by which suitably sized particles can be created.

These small particles which are aggregates of molecules (embryos) are continually formed and disrupted in the condensation process because of thermal and density fluctuations in the vapor. Unless the condition of supersaturation is very great, they do not survive and continue to grow to stable drops - they evaporate and disappear.

When the small embryos are present and an increase in vapor pressure results, the fuel composition is altered. Thus the temperature level required to achieve a given fuel vapor concentration is lowered - the "temperature flammability limits" have been shifted downward.

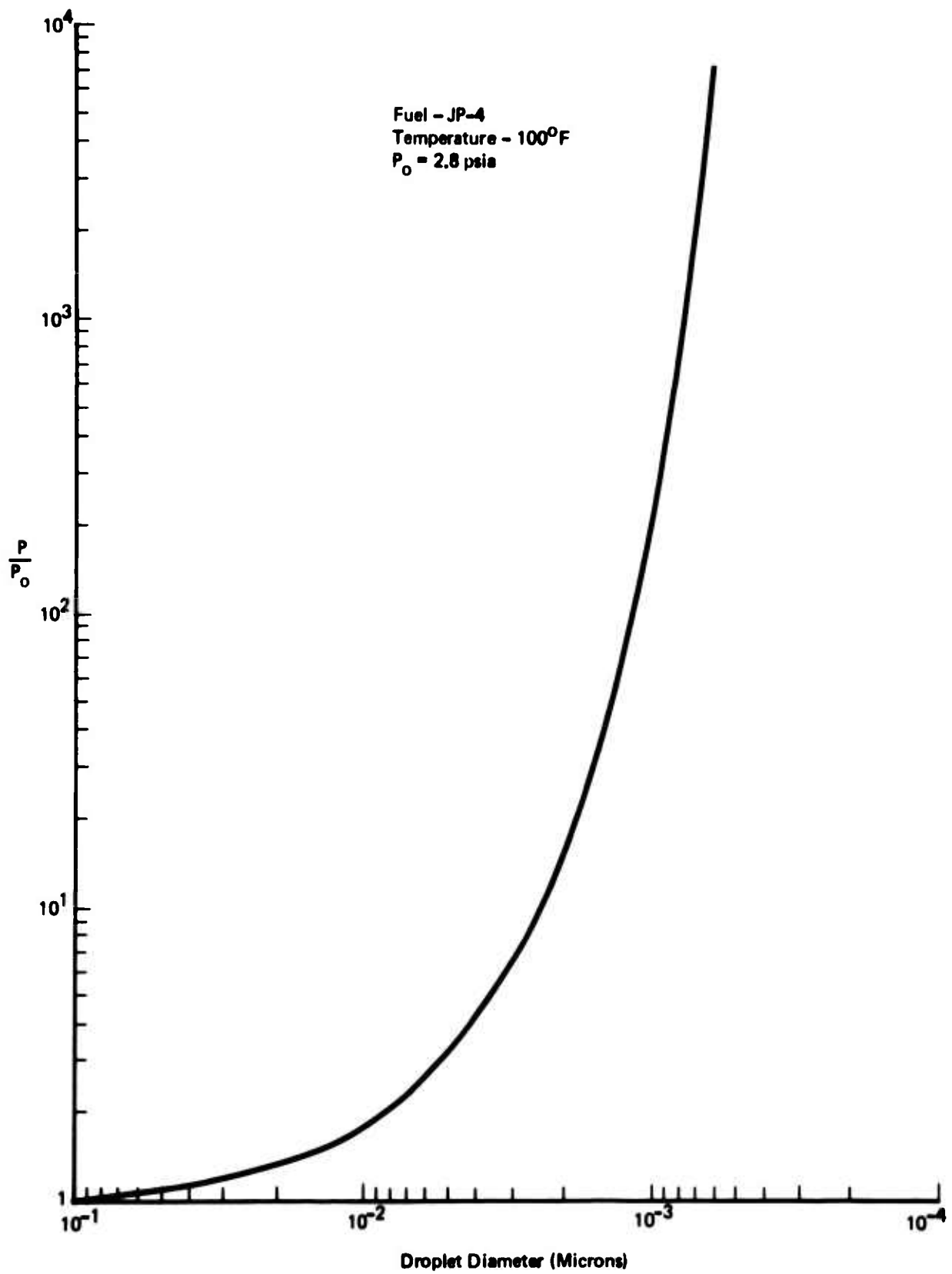


Figure 3. Calculation of Vapor Pressure From Fuel Mist Droplets.

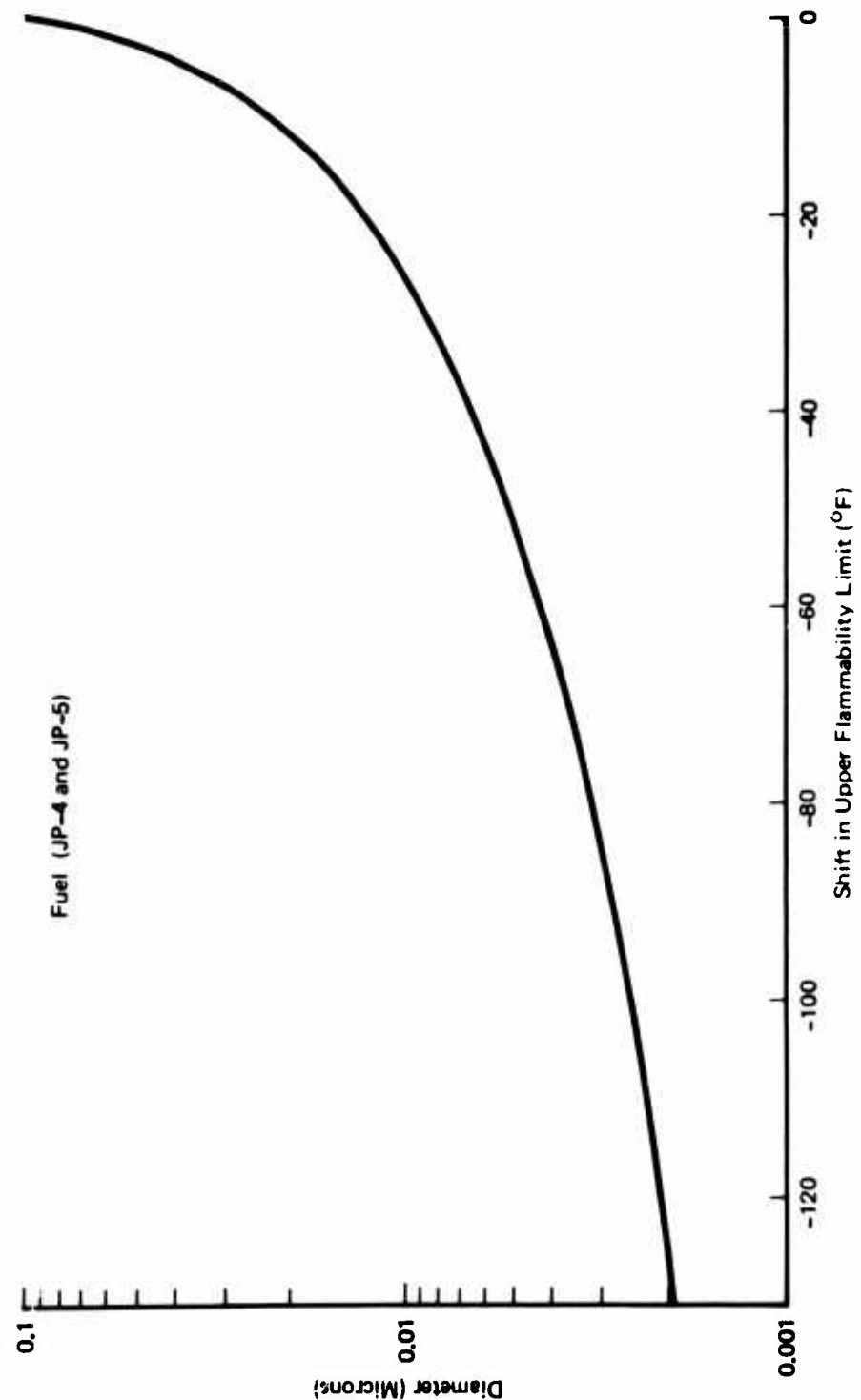


Figure 4. Calculation of Shift in Upper Flammability Limit Which Is Theoretically Possible as a Function of Mist Droplet Diameter.

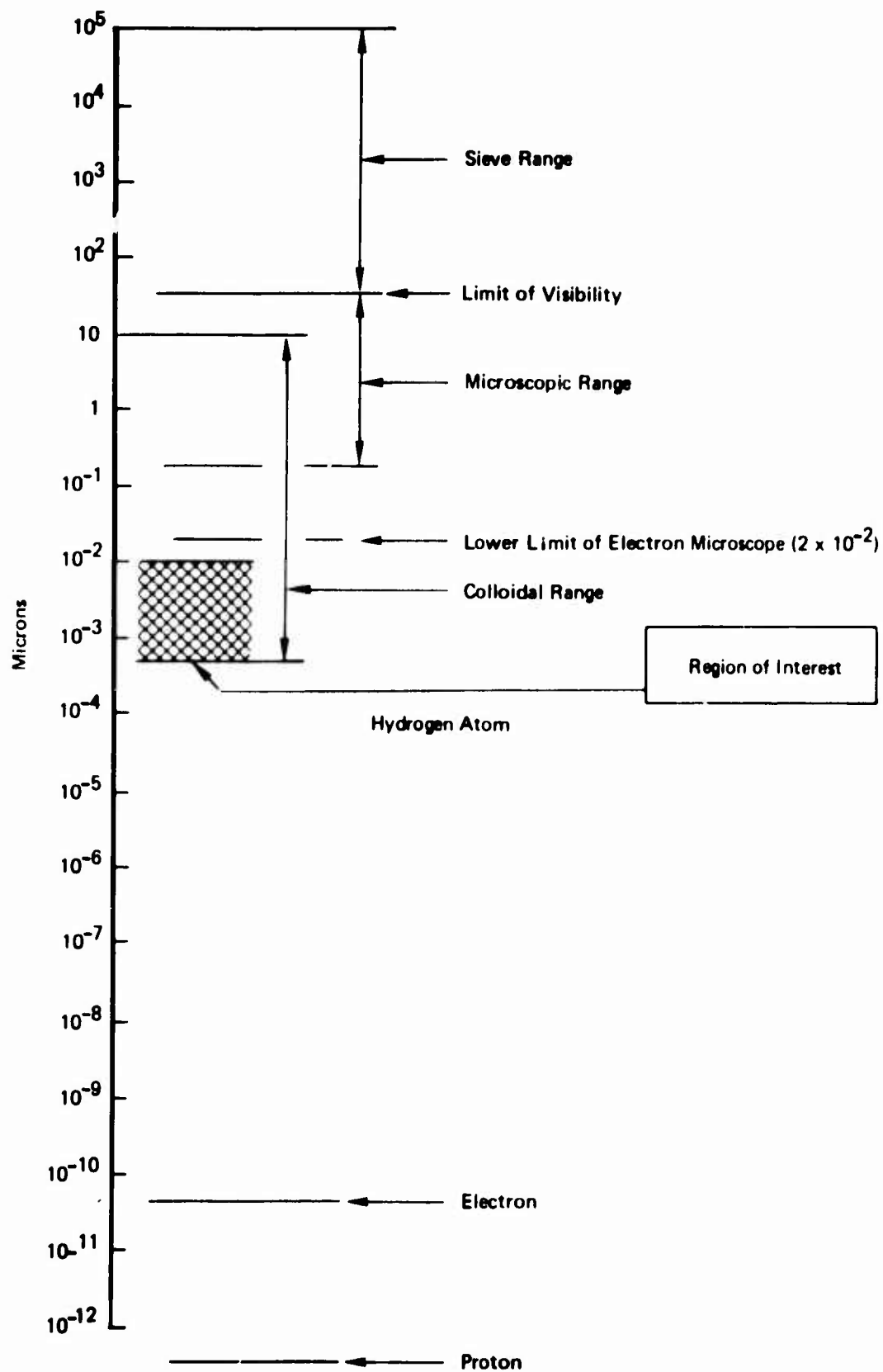


Figure 5. Size of Things.

Mechanism of Embryo Formation

Embryo formation requires a condition of temperature difference to create supersaturation in the vapor such that there is a tendency for condensation to occur. The condensation process involves the formation of clusters of molecules from single molecules. This must happen in the vapor phase, not on cold surfaces.

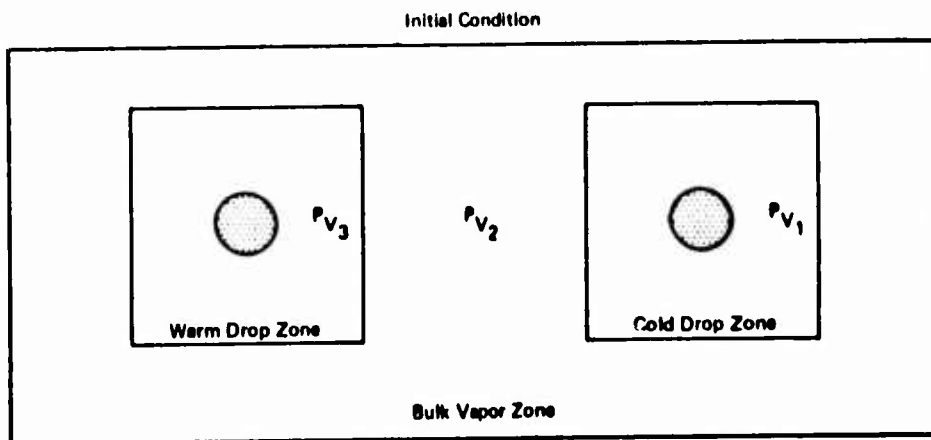
The fuel droplets sprayed into the vapor space by nozzles, which by themselves are much too large to affect vapor pressure, are the means by which a condition of supersaturation is created.

The alternatives available relative to the bulk vapor temperature are

1. Warm spray - one nozzle
2. Cool spray - one nozzle
3. Both warm and cool spray - two nozzles

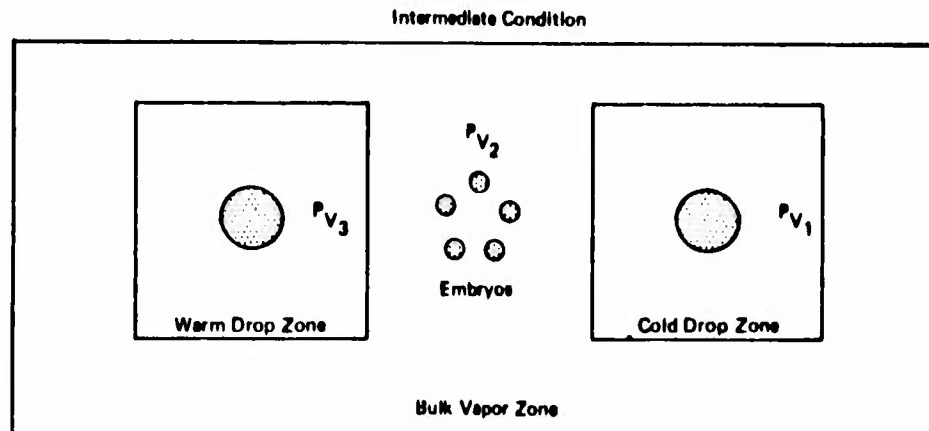
The alternatives 1 and 2 are of no interest because supersaturation cannot be established and maintained. In each case, the spray tends to bring the bulk vapor space to the same temperature as the spray. Thus supersaturation does not exist and embryo formation will not occur.

The use of both a warm spray and a cold spray will produce a constantly maintained condition of supersaturation. The sketches below are useful to illustrate the events which occur.



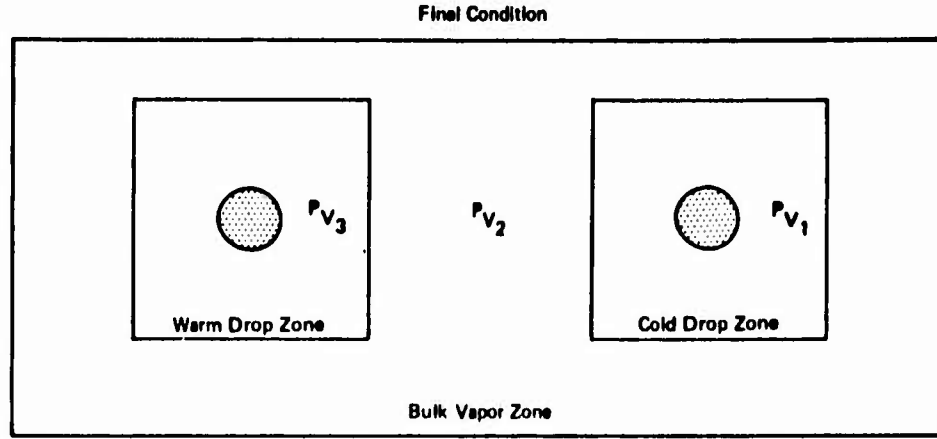
The local vapor pressures around the warm drop, in the bulk vapor, and around the cold drop are p_{v_3} , p_{v_2} , and p_{v_1} respectively.

Initially, as the individual warm and cold drops enter the region illustrated, $p_{v_3} > p_{v_2} > p_{v_1}$. Thus both the warm zone and the bulk vapor are supersaturated with respect to the cold zone. The warm zone is also supersaturated with respect to the bulk vapor. This condition is transitory, however, since the temperatures of both the warm and cold drops tend to approach that of the bulk vapor. An intermediate condition develops.



During this transition phase, the warm drop cools because vaporization occurs. Likewise, the cold drop warms because condensation occurs.

This vaporization and condensation cause molecules of vapor to move from the warm-drop zone and from the bulk-vapor zone to the cold-drop zone. At the same time, due to the supersaturation condition, embryos form in the bulk vapor zone. A condition then exists where $p_{v_3} < p_{v_2} > p_{v_1}$ and $p_{v_3} > p_{v_2}$. The embryos, which are too small to become stable droplets, then tend to disrupt and become vapor. Vapor molecules then move from the bulk vapor in both directions to the warm-drop zone and also the cold-drop zone. There is also movement of molecules from the warm-drop zone to the cold-drop zone. The final condition resulting from this process of vaporization and condensation is that $p_{v_3} = p_{v_2} = p_{v_1}$.



The process described above is repeated constantly as long as the spray flow rates are maintained.

The result is that localized supersaturation is constantly maintained throughout the vapor space, and embryo formation and disruption leading to increase of vapor pressure occur constantly.

A detailed thermodynamic treatment of embryos is presented in Appendix II, taken from Reference 4.

FUEL FOG TESTING

A test apparatus was developed and over 50 tests conducted under a variety of test conditions. These tests demonstrated the validity of the theory and led to the formulation of a set of spray conditions that provides ullage space inerting. Details of this test program follow.

Test Arrangement

A test arrangement was assembled with the capability of providing as wide a range of test conditions as practical. Included was the ability to change the bulk vapor temperature and the type, quality, quantity and temperature of one or two spray nozzles.

Alternate test arrangements are shown in Figures 6 and 7. Figure 6 shows the arrangement with air-brush nozzles. The air-brush system was included because this system had shown

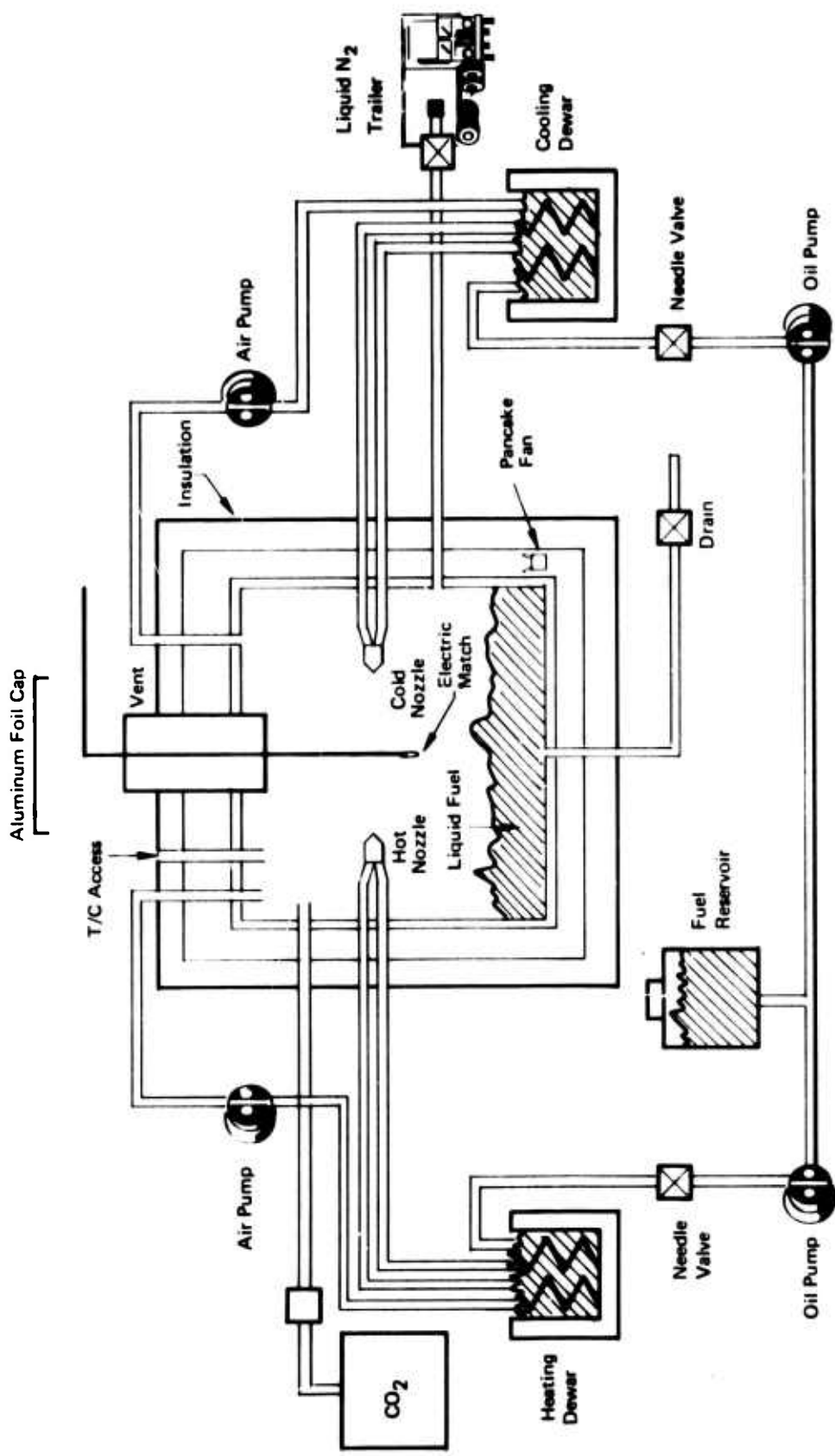


Figure 6. Test Arrangement - Air Brush Nozzles.

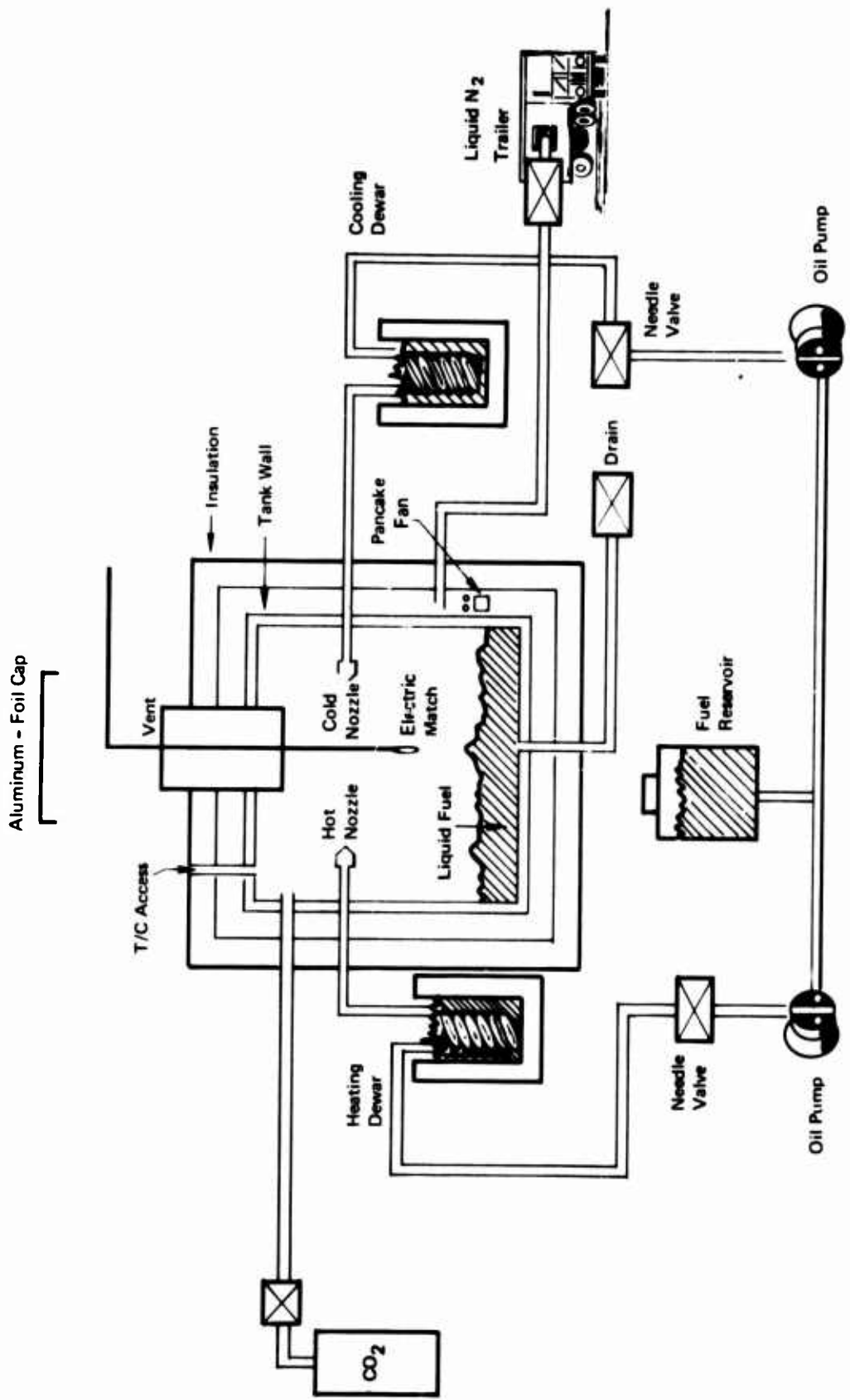


Figure 7. Test Arrangement - Oil Burner Nozzles.

promise during preliminary tests. However, its complexity made it undesirable for aircraft applications, and when simple nozzles were found to work, the air-brush system was rejected. Figure 7 shows the system used. The basic tank was a rectangular steel shell 18x24x24 inches high. Four 3-inch-diameter vent tubes extended through the tank top. A drain was provided that was periodically opened. However, a liquid surface was provided at the tank bottom during all tests. A 3-inch annular space was provided between the tank and an insulation layer.

The 4-inch layer of insulation was protected by an aluminum cover. Liquid nitrogen was introduced into the annular space to reduce the tank ullage temperature. A small fan was used to distribute the nitrogen around the tank. A CO₂ fire extinguisher was plumbed into the tank to suppress fires. JP-4 fuel was conditioned by pumping it from a reservoir through heating or cooling coils and to nozzles in the tank. The heating or cooling Dewars were filled with alcohol or acetone. For heating, a resistance (500-watt) heater was placed in the acetone; while for cooling, dry ice was placed in the alcohol or acetone. Aluminum foil caps were placed over the vents; they not only sealed the tank but provided an indication of pressure generated during a test. It was found that pressures varied from a slight dimpling of the caps to the blowing-off of one to all four of the caps.

One of the vents was used to insert the electric match. The match was inserted to the center of tank and ignited by application of 110 VAC with a 50-ohm resistor. The matches were constructed as shown in Figure 8. Two book-matches were glued together and a hole punched in each match shank. Ten-ohm-per-foot wire was run through the holes and wrapped around the match heads. The wires and match shanks were held in alligator clips, and the wire was bent so as to preclude condensate from collecting on the match heads.

When the vapor ignited during a test, the tank was purged for 15 minutes prior to setting up for the next test. (See Figures 9 and 10.) The purging was accomplished by inserting an air hose into one of the vent tubes.

Temperatures were measured by use of 12 thermocouples mounted in the tank, annular space, and heating and cooling Dewars. Spray temperatures were measured at the point where the minimum or maximum temperature was found. This point was found by moving the thermocouple around in the spray while monitoring the temperature. The point selected was in the edge of the spray about 1/2 inch in front of the nozzle. Monitoring was accomplished by means of a voltmeter.

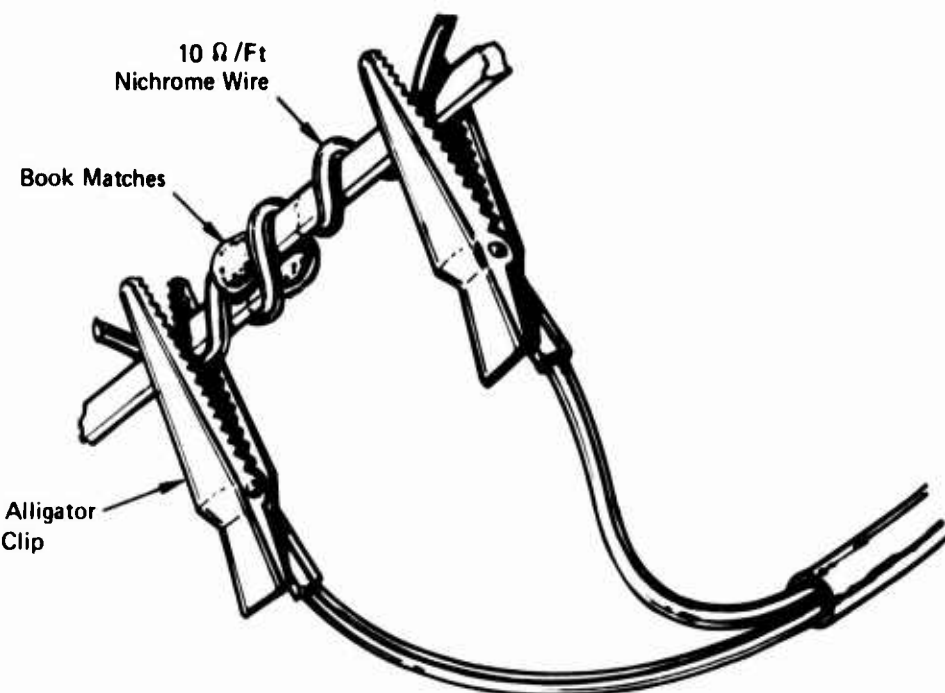


Figure 8. Electric Match.

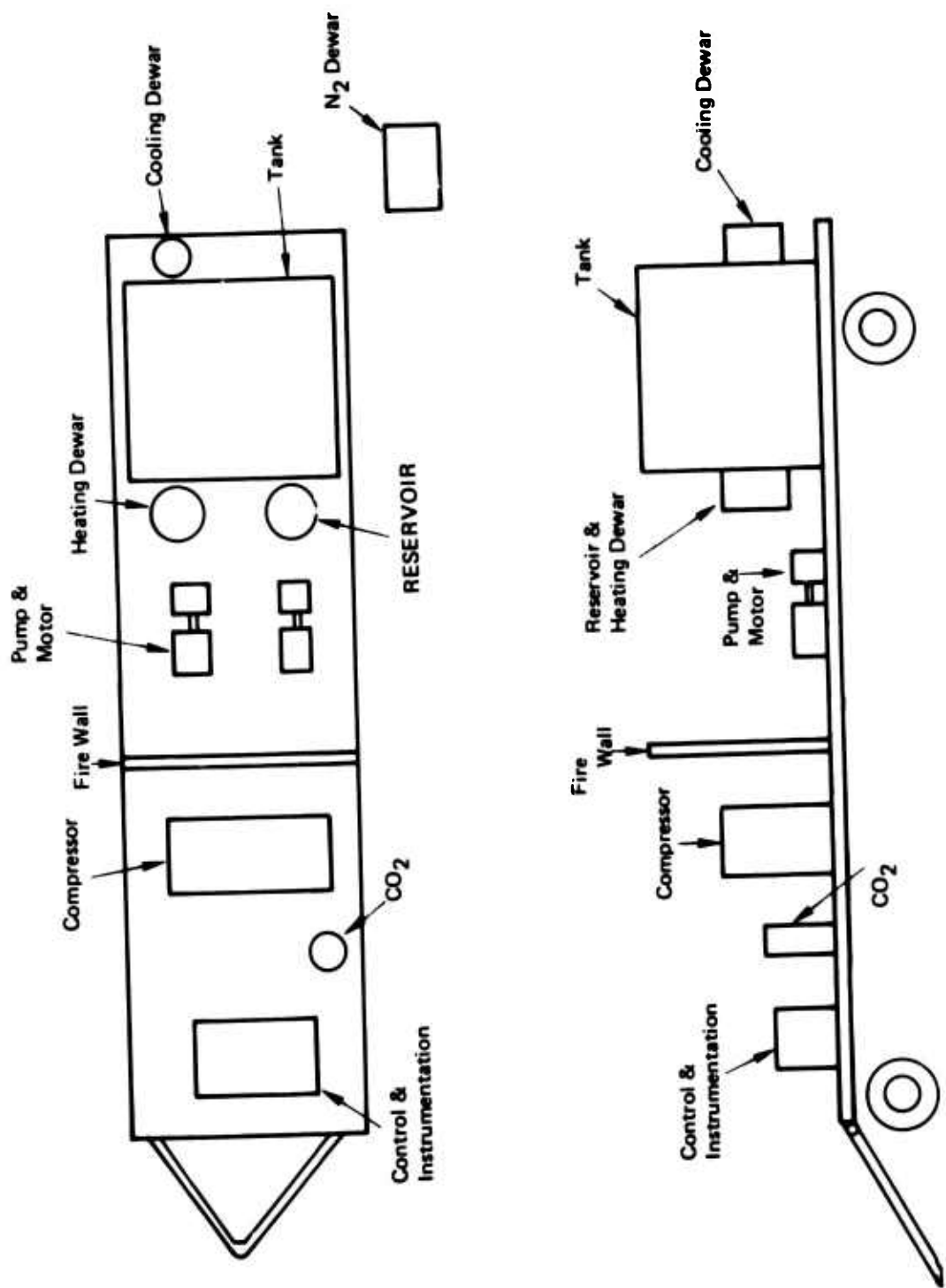


Figure 9. Test Arrangement Schematic.

Figure 10. Test Arrangement.



Test Results

Results of testing with a single nozzle are shown in Figure 11. These were the first tests made. Evaluation of the effectiveness of a single-nozzle configuration at that point in time was difficult because of the inconsistencies apparent in the test results. For example, at an ullage temperature of about 60° with a spray temperature 20° lower, results varied from no ignition to explosion. These results were interpreted at that time to indicate that if there was no ignition, it was probably due to some unknown effect in operation rather than an effect produced by operation of the single nozzle. It is very possible that the condensation phenomenon could have occurred sporadically because of subtle changes in the ullage space temperature gradients.

The remainder of the tests were made using a two-nozzle configuration with one spray warm and the other spray cold relative to the bulk ullage temperature. Results of tests with a 0.4-gph cold nozzle and a 0.4-gph hot nozzle are shown in Figure 12. These flow rates were not high enough to function below 55°. Previous work done in-house at Boeing had indicated that it becomes difficult to inert below this temperature.

The next test series was done with a 0.4-gph cold nozzle and a 1.0-gph hot nozzle. Results of these tests are shown in Figure 13. These results indicated that the configuration was still not adequate to function reliably in the ullage temperature region below 55°.

For the next series of tests, a 1.0-gph cold nozzle and a 1.0-gph hot nozzle were selected. Results of these tests are shown in Figure 14. This proved to be a reliable, effective configuration with reference to the normal explosive range. Two of these tests were made where both nozzles were "hot" relative to the bulk ullage temperature and two tests were made where both nozzles were "cold" relative to the bulk ullage temperature. Explosions occurred in all four cases.

In all cases where one nozzle was hot and the other cold, there was no explosion.

No attempt was made to establish minimum temperature difference limits. However, the data indicates that (for the system tested) this is no more than 5°F between 35° and the upper rich limit. The data obtained between 35° and the lower lean limit does not provide a basis for a similar conclusion.

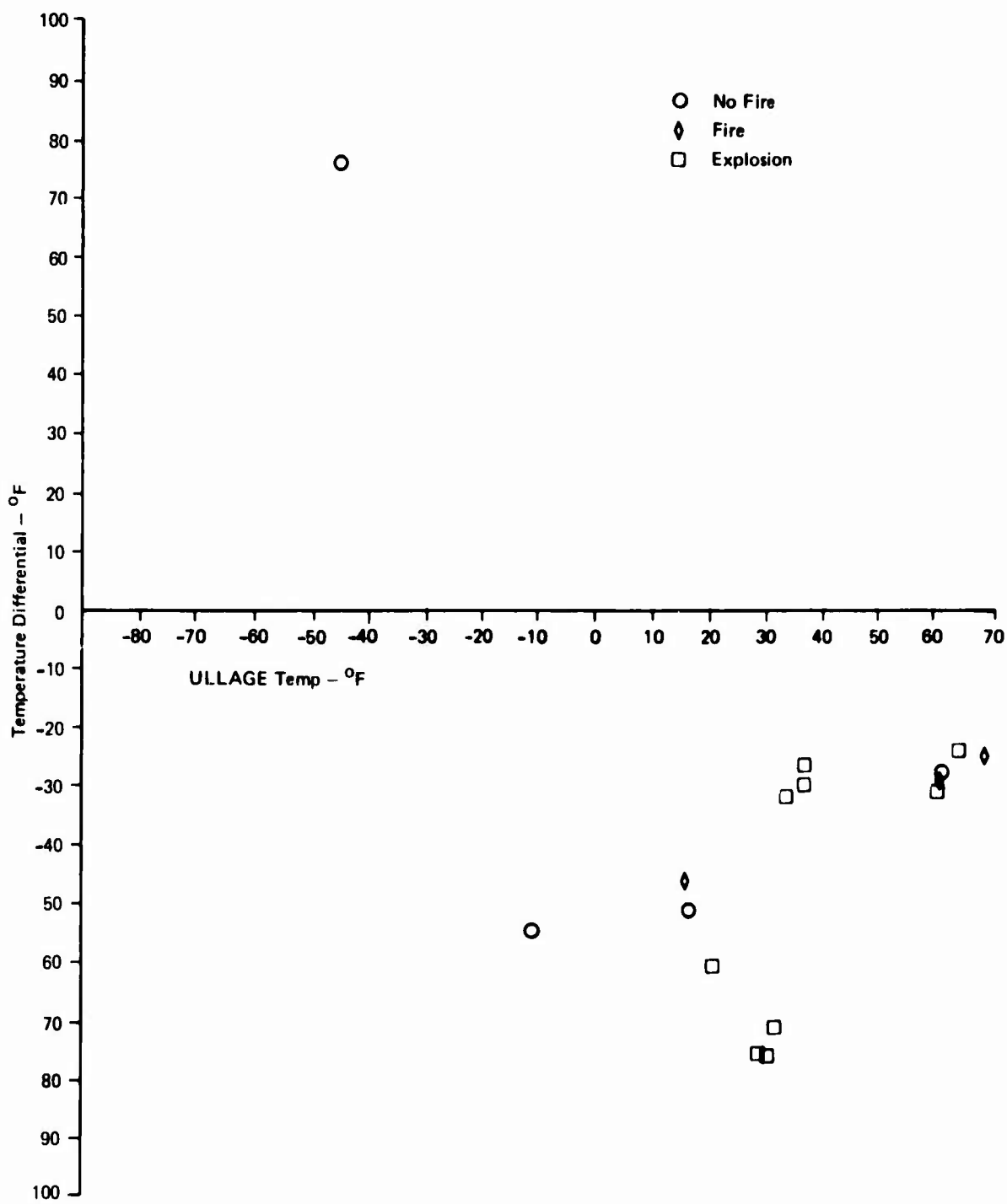


Figure 11. Single-Nozzle Test Results.

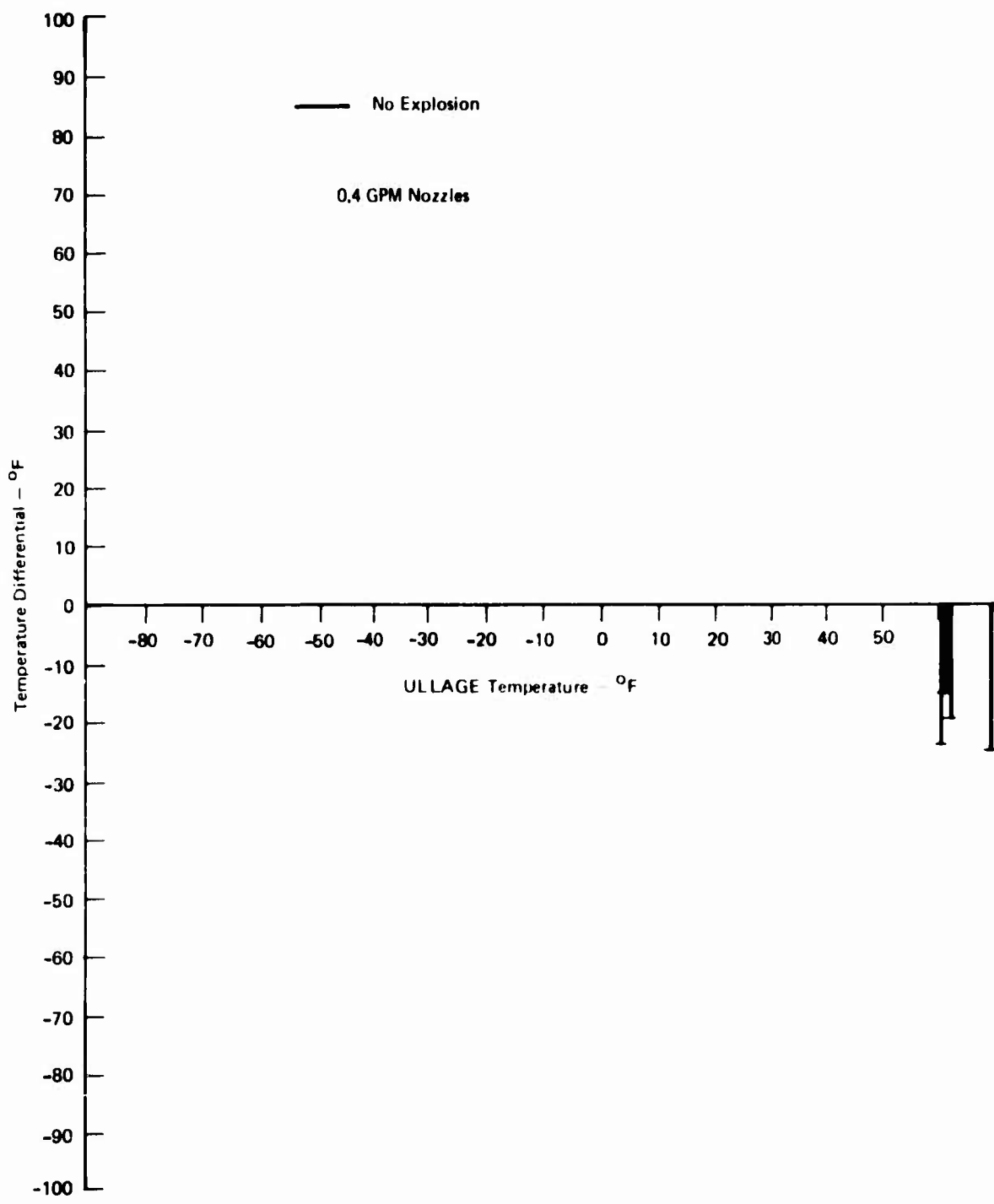


Figure 12. 0.4, 0.4 Nozzle Test Data.

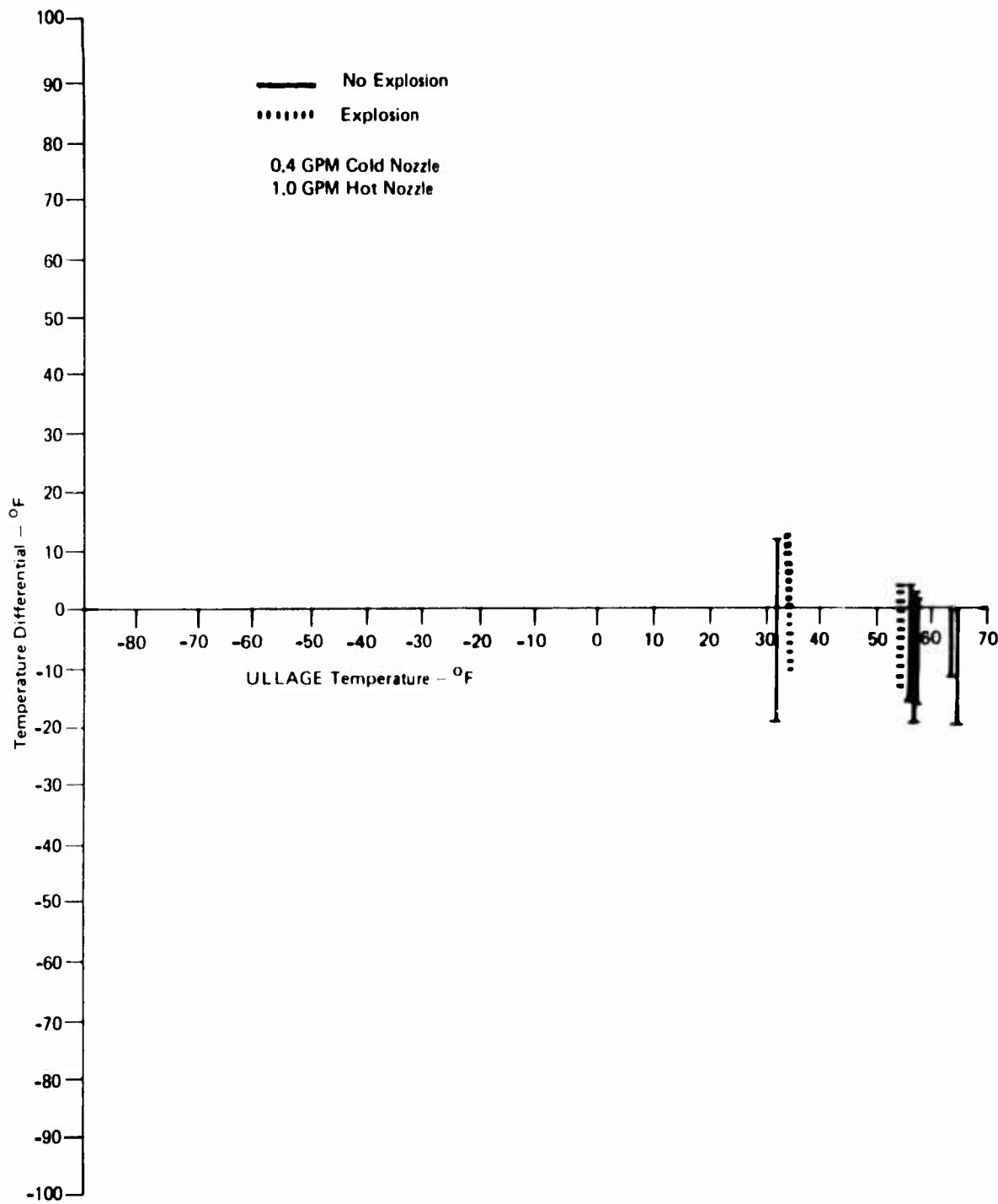


Figure 13. 0.4, 1.0 Nozzle Test Results.

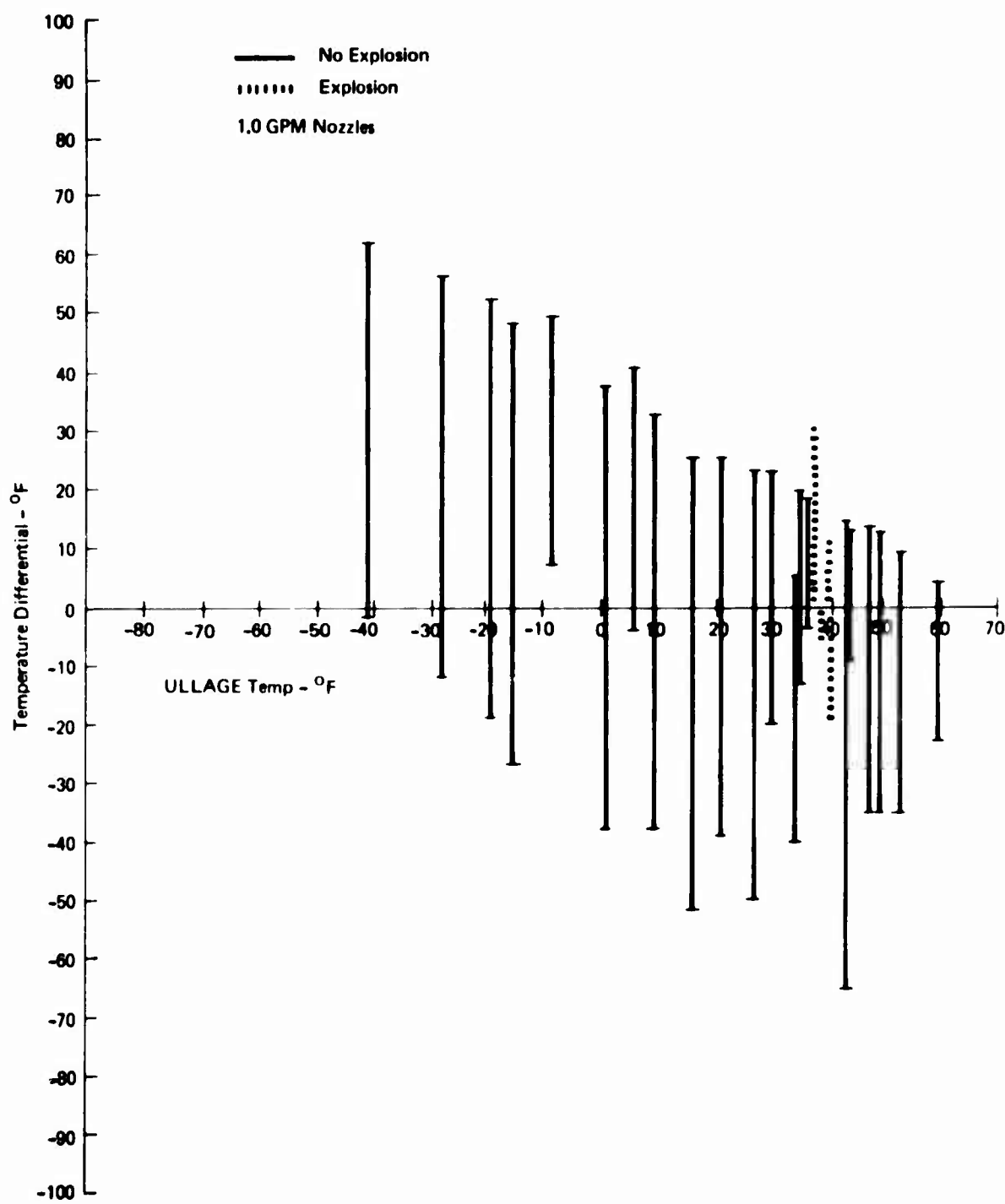


Figure 14. 1.0, 1.0 Nozzle Test Results.

The test apparatus operated in a very satisfactory manner. Desired temperatures were easy to establish and maintain. Ullage temperatures were controlled by changing the temperature in the annular space around the tank. It was found that the temperature in the center of the ullage space lagged the annular space temperature by no more than one or two degrees. This indicates that the mixing produced by the nozzle flow was very good. The consistency of the fog was examined by removing one of the vent covers and shining a light into the ullage space. The fog appeared light and "fluffy." The fog was thick enough to restrict vision to a few inches.

DESIGN APPLICATION

The AH-1G Cobra was selected as the Army aircraft for which to make a fuel fogging preliminary design. The Cobra fuel system is shown schematically in Figure 15. It is composed of two tanks with plumbing, valving and boost pumps. Each tank is roughly cubic in shape with forward and aft tanks having about 35 and 22 ft³ capacity, respectively.

Based on the Task II tests, spray conditions required would be:

- Forward Tank
 - 6 gal/hour hot
 - 6 gal/hour cold
 - Min. of 5°F temp differentials

- Aft Tank
 - 4 gal/hour hot
 - 4 gal/hour cold
 - Min. of 5°F temp differentials

In order to put the spray into a more inert range and to account for system variables, a temperature differential of 10°F will be used.

Pressurization for the spray can be obtained by bleed-off from the boost or engine feed pumps or from a special pump. The boost pumps do not supply pressure sufficiently high for best spray consistency. The engine feed pumps are adequate. However, an additional line from one engine to the fuel tanks must be installed. This adds weight and an additional vulnerable component. For this reason, the decision was made to use a special pump. Similar reasoning led to the selection of a special heat exchanger.

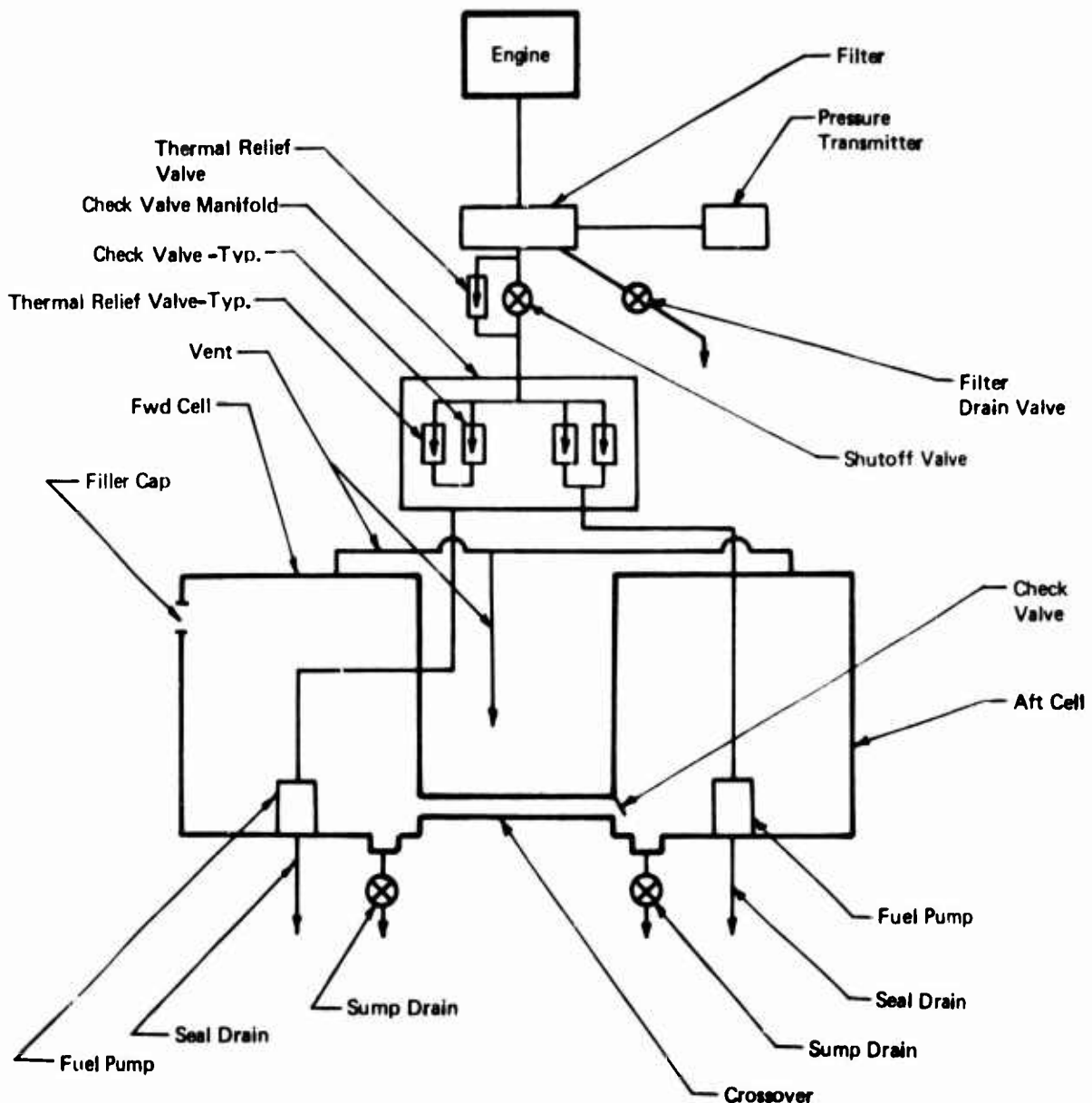


Figure 15. AH-1G Fuel System Schematic.

In the preliminary design, the pump and heat exchangers are packaged as a unit and powered by the same motor (Figure 16). The fuel is drawn through a filter at the bottom of the tank and forced through each side of the heat exchanger. The heat exchanger is a closed-cycle system with heat drawn from the cold-nozzle side added to the hot-nozzle side. Once through the heat exchanger, the fuel lines again split and are routed to nozzles near the top of each tank. Requirements for the various components are as follows:

Lines

Fuel lines should consist of 3/8-inch-diameter tubing on the suction side of the pump, 1/4-inch diameter between the pump and the first "T," and 1/8-inch tubing for the remaining lines.

Pressurization Pump

The fuel pressurization pump is mounted on the same shaft as the heat exchanger pump. The two pumps must then be designed to operate at the same speed. The pump must supply 20 gph at 100 psi. This will require 0.02 hp plus the power lost to heat and other inefficiencies. Total power required should be no more than 0.03 hp.

Heat Exchanger Pump

This pump, turning at the same rate as the fuel pressurization pump, must compress sufficient refrigerant to provide a minimum of 600 Btu/hr cooling capability. This would result in about 900 Btu/hr being ejected on the hot side.

Expansion Valve

The expansion valve allows the liquid refrigerant to expand into the gaseous phase. The valve must be sized to provide a temperature differential equivalent to 600 Btu/hr on the cold side.

Heat Exchangers

The total amount of fluid passing through the heat exchangers is small. Therefore, the small tubing (1/8 inch) provides a large surface area-to-volume ratio. For this reason, a simple tube-in-tube arrangement will be sufficient.

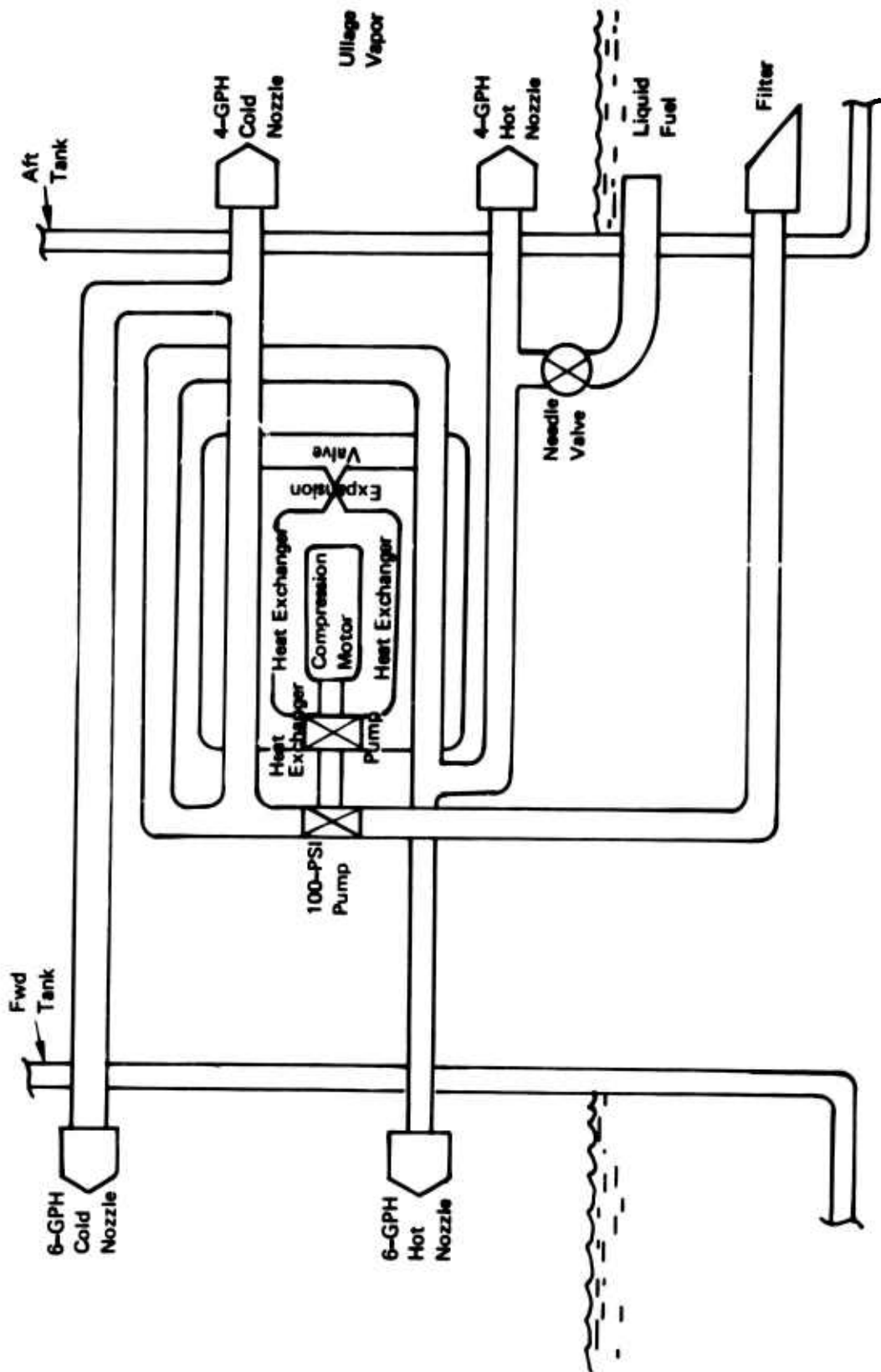


Figure 16. Fuel Fogger Preliminary Design.

Bypass Valve

The efficiency of refrigeration compressors is relatively low (on the order of 70%). For this reason, the temperature differential of the hot nozzle would be greater than that of the cold nozzle unless special provisions were made. This will be accomplished by allowing a certain amount of hot fuel to bypass the hot nozzle, thus increasing the hot side flow. The bypass valve will be a standard needle valve that can be adjusted to provide the desired temperatures at the time of system checkout.

Compressor Motor

The compressor motor must power both the pressurization pump and the heat exchanger pump. Combining these requirements and assuming a 70% efficiency, a motor requirement of 0.38 hp results. For a 28-VDC power supply, a current requirement of 10.1 amps results.

Nozzles

The nozzles are 6-gph oil-burner nozzles for the forward tank and 4-gph oil-burner nozzles for the aft tank.

Insulation

The fogging unit and all hot or cold lines require fuel-proof insulation such as urethane foam. This foam should be poured in place after installation. The foam thickness should be shaved to about 1 inch and the foam protected by a tape covering.

The best location for placing the fuel fogger unit is between the tanks. This will require installation of an electrical power and control cable. The unit itself will require a mounting space of about 4x6x12 inches. Overall weight is estimated to be about 10 pounds, including fuel line tubing. Location of the installation is shown in Figure 17.

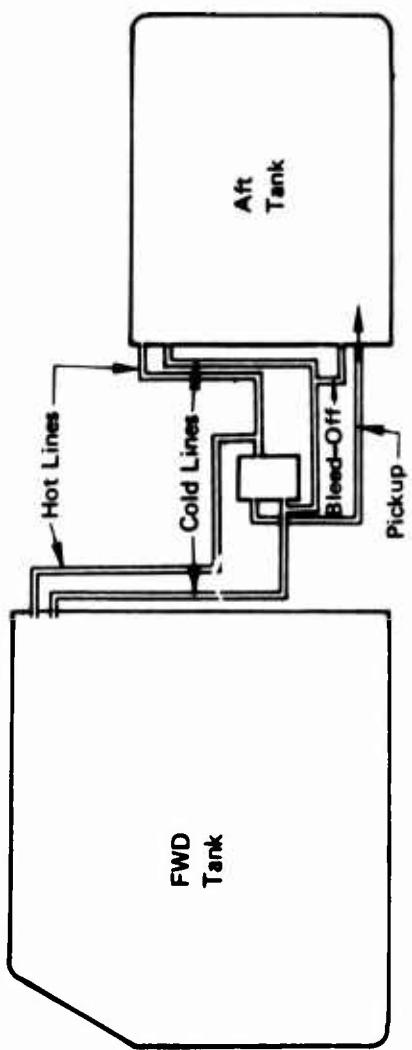


Figure 17. AH-1G Cobra Fuel Fogger Installation.

CONCLUSIONS

The conclusions of the program are as follows:

1. A combination of nozzles, spray flow rate, and spray temperature which provides inerting over the entire explosive range is possible.
2. Two spray nozzles are required, one at a temperature higher than and one lower than the bulk vapor temperature. The temperature differences required may be as small as 5°F.
3. Spray flow rate is a function of ullage space volume. For the 6-cubic-foot tank volume tested, 0.4-gph nozzles were inadequate while 1.0-gph nozzles were adequate.
4. Stratification is not a problem. Mixing caused by fuel spray flow maintains homogeneity. It is believed that homogeneity would also be obtained in an actual aircraft without further provision for mixing.
5. A fuel fogging system for the AH-1G Cobra would be about 10 pounds in weight and require 10 amps of 28-VDC power.

RECOMMENDATIONS

The testing demonstrated that it is feasible to use fuel fogging to inert fuel tank ullage spaces. The testing also provided sufficient quantitative data to enable a preliminary design to be developed for a fuel fog installation on an actual aircraft. However, a development program is still required in order to optimize the installation, to determine boundaries and limits of effectiveness, to assure that actual incendiary gun-fire conditions do not produce unforeseen problems, and that a practical device is available for temperature conditioning the fuel for the spray nozzles.

LITERATURE CITED

1. Kuhn, W. E., Editor, "Ultrafine Particles," John Wiley and Sons, NY (1963).
2. Dallavale, J. M., "Micrometrics," Pitman Publishing Corp., N.Y. (1948).
3. Moore, W. J., "Physical Chemistry," Prentice-Hall (1955).
4. Mason, B. J. D., Sc(Lond), "The Physics of Clouds," Oxford at the Clarendon Press (1957).

APPENDIX I
TEST DATA

The test data is shown in Table I. Two types of nozzles are shown. The designation "0-4" refers to an 80° A oil burner nozzle with a 0.4-gpm flow rate when used with a standard 100-psi oil burner pump. The other nozzle type was similar except that the flow rate was 1.0 gpm. All temperatures are in degrees Fahrenheit.

TABLE I FUEL FOG TEST DATA

Test Number	Spray Flow Rate (GPH)	Spray Temp (°F)	Ullage Temp (°F)	Temp Differential (°F)	Results			Comments
	Cold Side	Hot Side	Cold Side		Hot Side	No Burning	Mild Burning	
1	0.4	0.4	62	-24	0	•	•	
2	0.4	0.4	61	-15	-7	•	•	
3	0.4	0.4	67	-24	-17	•	•	
4	0.4	0.4	63	-25	-17	•	•	
5	0.4	0.4	62	-19	-17	•	•	
6	0.4	0.4	61	-28	-17	•	•	
7	0.4	0.4	60	-20	-17	•	•	
8	0.4	0.4	63	-12	-17	•	•	
9	0.4	0.4	64	-16	-17	•	•	
10	0.4	1.0	51	-30	-17	•	•	
11	0.4	1.0	44	-30	-17	•	•	
12	0.4	1.0	49	-30	-17	•	•	
13	0.4	1.0	49	-30	-17	•	•	
14	0.4	1.0	58	-30	-17	•	•	
15	0.4	1.0	59	-30	-17	•	•	
16	0.4	1.0	61	-30	-17	•	•	
17	0.4	1.0	43	-30	-17	•	•	
18	0.4	1.0	47	-30	-17	•	•	
19	0.4	1.0	34	-30	-17	•	•	
20	1.0	1.0	0	-30	-17	•	•	
21	1.0	1.0	10	-30	-17	•	•	
22	1.0	1.0	10	-30	-17	•	•	
23	1.0	1.0	10	-30	-17	•	•	
24	1.0	1.0	10	-30	-17	•	•	
25	1.0	1.0	10	-30	-17	•	•	
26	1.0	1.0	10	-30	-17	•	•	
27	1.0	1.0	10	-30	-17	•	•	
28	1.0	1.0	10	-30	-17	•	•	
29	1.0	1.0	10	-30	-17	•	•	
30	1.0	1.0	10	-30	-17	•	•	
31	1.0	1.0	10	-30	-17	•	•	
								Ullage T/C turned up
								Cold Nozzle T/C repositioned runs 20 - 29 recalibrated to make temps consistent

TABLE I (CONTINUED)

Test Number	Spray Flow Rate (GPH)		Spray Temp (°F)		Ullage Temp (°F)	Temp Differential (°F)	Results			Comments
	Cold Side	Hot Side	Cold Side	Hot Side			No Burning	Mild Burning	Burning	
32	1.0	1.0	-18	47	21	-39	26	33	49	May have had warm droplets from test no. 43 Very slight burn
33	1.0	1.0	-28	43	10	-38	38	53	62	• • • • • • • • • • • • • • • • • •
34	1.0	1.0	-27	38	-15	-27	49	57	76	• • • • • • • • • • • • • • • • • •
35	1.0	1.0	-21	35	-19	53	14	19	24	• • • • • • • • • • • • • • • • • •
36	1.0	1.0	-28	41	-12	57	62	76	82	• • • • • • • • • • • • • • • • • •
37	1.0	1.0	-21	47	-10	-	14	19	20	30
38	1.0	1.0	-55	60	-23	5	10	14	20	30
39	1.0	1.0	-47	44	9	9	13	18	24	31
40	1.0	1.0	-55	38	38	8	13	18	24	32
41	1.0	1.0	-55	50	50	8	13	18	24	32
42	1.0	1.0	-53	53	53	8	13	18	24	32
43	1.0	1.0	-53	48	48	6	9	13	18	24
44	1.0	1.0	-53	38	38	6	9	13	18	24
45	1.0	1.0	-53	32	32	2	7	12	17	22
46	1.0	1.0	1.0	1.0	1.0	18	22	27	32	37
47	1.0	1.0	1.0	1.0	1.0	13	18	22	27	32
48	1.0	1.0	1.0	1.0	1.0	10	15	20	25	30
49	1.0	1.0	1.0	1.0	1.0	7	12	17	22	27
50	1.0	1.0	1.0	1.0	1.0	4	9	14	19	24
51	1.0	1.0	1.0	1.0	1.0	1	6	11	16	21
52	1.0	1.0	1.0	1.0	1.0	1	6	11	16	21
53	1.0	1.0	1.0	1.0	1.0	1	6	11	16	21
54	1.0	1.0	1.0	1.0	1.0	1	6	11	16	21
55	1.0	1.0	1.0	1.0	1.0	1	6	11	16	21
56	1.0	1.0	1.0	1.0	1.0	1	6	11	16	21

(○) Cold Nozzle Only
 (◎) Hot Nozzle Inoperative
 (●) Hot Nozzle Only

APPENDIX II
THERMODYNAMIC TREATMENT OF CONDENSATION-FORMED EMBRYOS
(Reference 4)

Embryos are aggregates of molecules which are continually formed and disrupted because of microscopic thermal and density fluctuations in the vapor. Unless the condition of supersaturation is great enough, they do not survive and continue to grow - they evaporate and disappear.

THERMODYNAMIC DERIVATION OF KELVIN'S FORMULA

Consider a closed system at a temperature T , containing vapor at a pressure p , and one embryo of liquid, radius r , consisting of g molecules.

The Gibbs potential per molecule in the vapor phase is ϕ_a and in the liquid phase is ϕ_b . Assume that the embryo has been formed by condensation of g molecules of vapor. The change in free energy then is

$$\phi = (\phi_b - \phi_a)g + 4\pi r^2 \sigma_{LV} \quad (1)$$

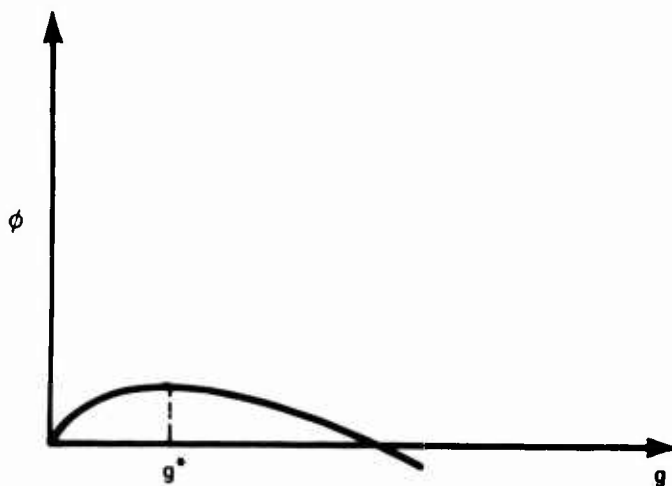
$$= (\phi_b - \phi_a)g + \alpha g^{2/3} \quad (2)$$

where α is a constant such that

$$\alpha g^{2/3} = 4\pi r^2 \sigma_{LV}$$

The second term on the right of equations (1) and (2) is the surface free-energy term, which makes an important contribution to ϕ because of the large surface-to-volume ratio of the droplet.

The way in which free-energy ϕ varies with the size of an embryo is shown in the figure below for the supersaturated vapor condition where $\phi_a > \phi_b$.



There is a maximum free energy of the system when g has a certain critical value g^* . When the embryo has this critical size it is in equilibrium with the vapor, but the equilibrium is unstable. If the embryo exceeds this critical size, it will grow with a decrease in free energy, thus tending to become larger still.

However, if the vapor phase is thermodynamically stable where $\phi_a < \phi_b$, embryos of the new phase reach only a relatively small size (below g^*) and then disappear.

The condition for equilibrium between the embryo and the vapor is found by differentiating equation (2). It is found that

$$\frac{d\phi}{dg} = 0 \text{ when}$$

$$\phi_b - \phi_a = - \frac{2\alpha}{3g^{1/3}} = - \frac{8\pi\sigma LVr^2}{3g} \quad (3)$$

but

$$g = \frac{4\pi r^3 N \rho L}{3M} \quad (4)$$

where N = Avogadro's number

M = Molecular weight

Combining (3) and (4),

$$\phi_a - \phi_b = \frac{2M\sigma}{N\rho} \frac{LV}{r^*} \quad (5)$$

where r^* = radius of an embryo containing g^* molecules

Now assume that the vapor pressure is changed by a small amount dp at constant temperature with a corresponding small change in free energy per molecule of $d\phi_a$. Then if v_a is the volume occupied by a molecule in the vapor phase,

$$d\phi_a = v_a dp$$

For the same change of pressure in the liquid phase, the free-energy change per molecule is

$$d\phi_b = v_b dp$$

Therefore, we can write

$$d(\phi_a - \phi_b) = (v_a - v_b) dp \approx \frac{kT}{p} dp \quad (6)$$

where k = Boltzmann constant, the molecular gas constant. We can do this because $v_b \ll v_a$.

Integration of equation (6) over a pressure range of p_∞ to p gives

$$\phi_a - \phi_b = kT \ln \frac{p}{p_\infty} = kT \ln S \quad (7)$$

where S is the saturation ratio.

Substituting the value of $\phi_a - \phi_b$ from equation (7) into (5) gives

$$\ln \frac{p}{p_\infty} = \frac{2M\sigma}{\rho_L R T r^*} \frac{LV}{\rho} \quad (8)$$

which is Kelvin's equation.

STATISTICAL EQUILIBRIUM BETWEEN EMBRYOS OF DIFFERENT SIZES

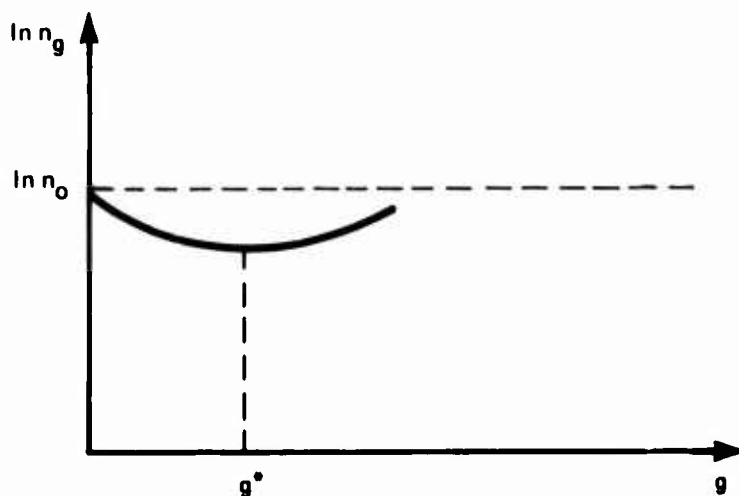
According to equation (2), the system is in true equilibrium only when $g = 0$ (minimum value of ϕ).

For small finite values of ϕ , there is always a small probability, $e^{-\phi}/kT$, that the system will be in a nonequilibrium state because of microscopic temperature and density fluctuations.

If, in any system consisting of n_0 molecules, there are n_g embryos each consisting of g molecules, then the most probable distribution is shown by Frenkel to be given by

$$n_g = n_0 \exp(-\phi/kT) = n_0 \exp \left[g \ln S - \frac{\alpha g^{2/3}}{kT} \right] \quad (9)$$

The way in which the number of embryos of different sizes varies with the number of molecules g in each for a supersaturated system is shown in the following figure.



n_g has a minimum value when the number of molecules in the embryo has a critical value g^* corresponding to the critical radius r^* in (8).

For the following analysis, assume that the equilibrium distribution given by equation (9) has been set up. We will examine the microscopic balancing conditions for dynamic equilibrium between embryos of size g , embryos of size $g-1$, and the vapor.

The number of molecules β_g striking an embryo of size g , radius r , per second is

$$\beta_g = \frac{4\pi r^2 N_p}{(2\pi MRT)^2} \quad (10)$$

It is assumed that all the vapor molecules striking an embryo are captured by it. Therefore, the number of embryos of size $g-1$ becoming embryos of size g per second is

$$\beta_{g-1} n_{g-1}$$

Similarly, if α_g is the number of molecules evaporating from an embryo of size g per second, then the number of embryos of size g becoming embryos of size $g-1$ per second is

$$\alpha_g n_g$$

For dynamic equilibrium we have

$$\beta_{g-1} n_{g-1} = \alpha_g n_g \quad (11)$$

Let ξ be α_g / β_{g-1} .

Then

$$\xi = \frac{\alpha_g}{\beta_{g-1}} = \frac{n_{g-1}}{n_g}$$

and

$$\ln \xi = \ln n_{g-1} - \ln n_g = \frac{-d}{dg} \ln n_g \quad (12)$$

Substitution from (9) gives

$$\xi = \exp \left[-\ln S + \frac{2\alpha}{g^{1/3} 3kT} \right] \quad (13)$$

Equation (13) is a very important one because it gives the ratio of the number of molecules evaporating from an embryo and the number hitting an embryo one size smaller.

For very small embryos, equation (13) shows that ξ is large (because $\frac{\alpha}{g^{1/3}}$ is proportional to $\frac{1}{r}$). A large value of ξ indicates a tendency for the embryos to evaporate rather than to grow. In this region of the equilibrium distribution, dynamic

equilibrium is maintained because, according to equation (9),
there are more small embryos than large ones.

Therefore, for the condensation-formed fuel fog concept to be effective, the value of ξ must be large.

Equation (13) has been calculated for JP-4 as a function of temperature for two sizes of embryo. The results are shown in Figure 18.

This data shows very well that the fog concept will be much more effective at lower temperatures.

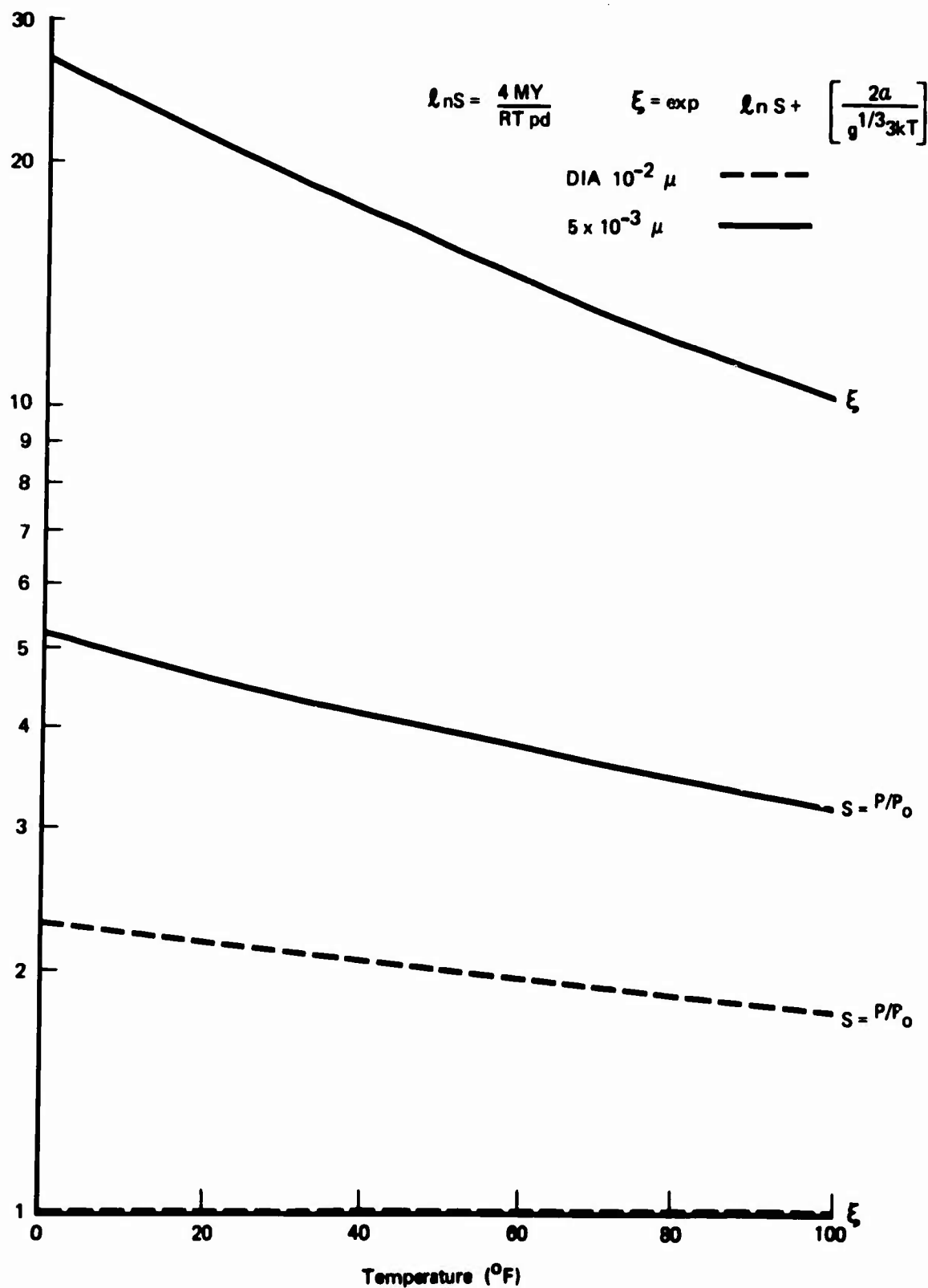


Figure 18. Comparison of Evaporation Potential for Two Different Embryo Diameters.